

# Ca<sup>2+</sup> /calmodulin-dependent protein kinase II (CaMKII) is activated by calmodulin with two bound calciums

Julia M. Shifman\*<sup>†‡</sup>, Mee H. Choi\*<sup>§</sup>, Stefan Mihalas\*, Stephen L. Mayo\*<sup>†¶</sup>, and Mary B. Kennedy\*<sup>¶</sup>

\*Division of Biology and <sup>†</sup>Howard Hughes Medical Institute, California Institute of Technology, Pasadena, CA 91125

Contributed by Stephen L. Mayo, July 27, 2006

Changes in synaptic strength that underlie memory formation in the CNS are initiated by pulses of Ca<sup>2+</sup> flowing through NMDA-type glutamate receptors into postsynaptic spines. Differences in the duration and size of the pulses determine whether a synapse is potentiated or depressed after repetitive synaptic activity. Calmodulin (CaM) is a major Ca<sup>2+</sup> effector protein that binds up to four Ca<sup>2+</sup> ions. CaM with bound Ca<sup>2+</sup> can activate at least six signaling enzymes in the spine. In fluctuating cytosolic Ca<sup>2+</sup>, a large fraction of free CaM is bound to fewer than four Ca<sup>2+</sup> ions. Binding to targets increases the affinity of CaM's remaining Ca<sup>2+</sup>-binding sites. Thus, initial binding of CaM to a target may depend on the target's affinity for CaM with only one or two bound Ca<sup>2+</sup> ions. To study CaM-dependent signaling in the spine, we designed mutant CaMs that bind Ca<sup>2+</sup> only at the two N-terminal or two C-terminal sites by using computationally designed mutations to stabilize the inactivated Ca<sup>2+</sup>-binding domains in the "closed" Ca<sup>2+</sup>-free conformation. We have measured their interactions with CaMKII, a major Ca<sup>2+</sup>/CaM target that mediates initiation of long-term potentiation. We show that CaM with two Ca<sup>2+</sup> ions bound in its C-terminal lobe not only binds to CaMKII with low micromolar affinity but also partially activates kinase activity. Our results support the idea that competition for binding of CaM with two bound Ca<sup>2+</sup> ions may influence significantly the outcome of local Ca<sup>2+</sup> signaling in spines and, perhaps, in other signaling pathways.

postsynaptic | protein design | synaptic plasticity | microdomains

Calmodulin (CaM) is a Ca<sup>2+</sup> effector protein comprised of two Ca<sup>2+</sup>-binding lobes connected by a short linker region. Each lobe contains two EF hands that bind Ca<sup>2+</sup> with low micromolar affinity. CaM mediates a host of regulatory effects of Ca<sup>2+</sup> despite the fact that the Ca<sup>2+</sup> concentration in the cytosol rarely reaches a level expected to saturate all four Ca<sup>2+</sup>-binding sites on free CaM (1). This sensitivity is possible because association of CaM with its targets stabilizes its Ca<sup>2+</sup>-bound conformation and, therefore, increases its affinity for Ca<sup>2+</sup> (2–4). When CaM with two Ca<sup>2+</sup> ions bound to either the N- or the C-terminal lobe associates with a target, the affinity of the remaining lobe for Ca<sup>2+</sup> increases, often by at least one order of magnitude, causing high positive cooperativity of Ca<sup>2+</sup> binding (5). Because of this property, we predict that when Ca<sup>2+</sup> concentrations fluctuate in the cytosol, competition among targets for binding of CaM will depend on their affinities for CaM with one or two bound Ca<sup>2+</sup> and also on the magnitude of cooperativity induced by binding to each target.

In the CNS, Ca<sup>2+</sup> influx into postsynaptic spines of excitatory glutamatergic synapses is a key determinant of changes in synaptic strength that underlie memory formation. The direction of the change in strength is determined by the timing between release of glutamate at the synapse and depolarization of the postsynaptic membrane, caused, for example, by a back-propagating action potential. This timing controls the duration and extent of Ca<sup>2+</sup> influx through NMDA-type glutamate receptors into the spine. Relatively large increases of a few micromolars in Ca<sup>2+</sup> concentration occurring over 2 to 3 sec induce long-term potentiation of the synapse. In contrast, smaller changes of a few hundred nanomolars, lasting over several seconds to 1 min, induce long-term depression of the synapse (6–10).

How might these slight differences in Ca<sup>2+</sup> influx produce such dramatic differences in regulation of the synapse? Ca<sup>2+</sup> that flows into a spine through activated NMDA receptors binds to CaM and to several other Ca<sup>2+</sup>-binding proteins. Ca<sup>2+</sup> binding to CaM enables its interaction with, and regulation of, several postsynaptic proteins. Two prominent targets of Ca<sup>2+</sup>/CaM are Ca<sup>2+</sup>/calmodulin-dependent protein kinase II (CaMKII) (11, 12) and calcineurin, a protein phosphatase (13, 14). The apparent affinities of these two proteins for Ca<sup>2+</sup>/CaM are quite different when measured at saturating Ca<sup>2+</sup> concentrations (>200 μM). CaMKII is half maximally activated at ≈40–80 nM CaM (15–17), whereas calcineurin is half maximally activated at 1–10 nM CaM (18, 19). This severalfold difference in affinity for Ca<sup>2+</sup>/CaM has been invoked to explain the different synaptic effects of high and low Ca<sup>2+</sup> fluxes (20). However, an accurate description of the critical initial steps of Ca<sup>2+</sup> signaling in spines requires a precise understanding of how different CaM targets in the spine compete for Ca<sup>2+</sup> under conditions in which quantities of Ca<sup>2+</sup>/CaM are limited and concentrations of Ca<sup>2+</sup> are fluctuating.

In the work reported here, we focus on understanding interactions between CaM and CaMKII when the concentrations of Ca<sup>2+</sup> or CaM are limiting. CaMKII is a dodecameric oligomer of catalytic subunits, each of which can bind one CaM (21–23). Binding of CaM to an individual subunit activates its kinase activity allowing the subunit to phosphorylate other proteins. In addition, binding of two CaM molecules to two adjacent subunits within a holoenzyme allows autophosphorylation of one or both of the subunits at Thr-286 (24). This autophosphorylation renders the subunit constitutively active and it remains so until the phosphate is removed by a protein phosphatase (25, 26). Activation and autophosphorylation of CaMKII has been shown to be crucial for induction of long-term potentiation (27).

To measure the affinity of CaMKII for CaM with less than four bound Ca<sup>2+</sup> ions, we designed a mutant CaM that binds Ca<sup>2+</sup> only at N-terminal sites (CaM-N<sup>WT</sup>) and a mutant CaM that binds Ca<sup>2+</sup> only at C-terminal sites (CaM-C<sup>WT</sup>). To closely mimic conformations of CaM that would exist in the cytosol, we used computationally designed mutations to stabilize the inactivated Ca<sup>2+</sup>-binding domains in the "closed," Ca<sup>2+</sup>-free con-

Author contributions: J.M.S. and M.H.C. contributed equally to this work; J.M.S., M.H.C., S.M., S.L.M., and M.B.K. designed research; J.M.S., M.H.C., and S.M. performed research; J.M.S., M.H.C., S.M., S.L.M., and M.B.K. analyzed data; and J.M.S., M.H.C., and M.B.K. wrote the paper.

The authors declare no conflict of interest.

Abbreviations: CaMKII, Ca<sup>2+</sup>/calmodulin-dependent protein kinase II; CaM, calmodulin; CaM-N<sup>WT</sup>, mutant CaM that binds Ca<sup>2+</sup> only at N-terminal sites; CaM-C<sup>WT</sup>, mutant CaM that binds Ca<sup>2+</sup> only at C-terminal sites; CaMKII-cbp, peptide having the sequence of the CaM-binding domain of CaMKII; CaM2C, WT CaM with two Ca<sup>2+</sup> ions bound at its C terminus; CaM2N, WT CaM with two Ca<sup>2+</sup> ions bound at its N terminus; CaM4, WT CaM with Ca<sup>2+</sup> ions bound at all four sites.

<sup>†</sup>Present address: Department of Biological Chemistry, The Alexander Silberman Institute of Life Sciences, Hebrew University of Jerusalem, Jerusalem 91904, Israel.

<sup>§</sup>Present address: Department of Neurobiology, School of Medicine, University of Pittsburgh, E1440 BST, 3500 Terrace Street, Pittsburgh, PA 15261.

<sup>¶</sup>To whom correspondence should be addressed. E-mail: kennedym@its.caltech.edu or steve@mayo.caltech.edu.

© 2006 by The National Academy of Sciences of the USA



**Table 1. Computationally designed N- and C-terminal mutant CaMs**

CaMs	Designed positions																			
	Site 1					Site 2					Site 3					Site 4				
	20	22	24	27	31	56	58	60	62	67	93	95	97	100	104	129	131	133	135	140
CaM WT	D	D	D	I	E	D	D	N	T	E	D	D	N	I	E	D	D	D	Q	E
CaM-C <sup>WT</sup>	<b>T</b>	<b>K</b>	<b>Q</b>	<b>I</b>	<b>E</b>	<b>S</b>	<b>D</b>	<b>E</b>	<b>I</b>	<b>K</b>	-	-	-	-	-	-	-	-	-	-
CaM-N <sup>WT</sup>	-	-	-	-	-	-	-	-	-	-	<b>A</b>	<b>R</b>	<b>D</b>	<b>M</b>	<b>E</b>	<b>R</b>	<b>D</b>	<b>N</b>	<b>E</b>	<b>N</b>

All CaM residues that directly coordinate Ca<sup>2+</sup> ions with their side chains (positions 20, 22, 24, 31, 56, 58, 60, and 67 for the N-terminal domain and 93, 95, 97, 104, 129, 131, 133, and 140 for the C-terminal domain) were included in the optimization. Residues 62 and 135 also were included because they coordinate Ca<sup>2+</sup> ions with their backbone carbonyls. Residues 27 and 100, which do not coordinate Ca<sup>2+</sup> ions, but are in close proximity to the ion and help define the Ca<sup>2+</sup>-binding loop, also were optimized. Bold lettering shows mutations with respect to the WT CaM sequence. -, positions were not included in the calculation for the mutant CaM indicated.

CaM adopts a closed conformation (33, 37, 38) in which it is not able to interact with most of its targets (Fig. 2A). Binding of Ca<sup>2+</sup> to CaM causes a reorientation of helices inside the globular domains and a consequent exposure of patches of hydrophobic residues important for target recognition (34) (Fig. 2B). A shift toward this “open” CaM conformation is believed to be a prerequisite for interactions with many CaM-regulated proteins (1, 32, 39). Binding to most targets, including the CaM-binding domain of CaMKII (CaMKII-cbp), induces a conformation in which CaM wraps around the target domain, resulting in a coil-to-helix transition in the target (35, 40) (Fig. 2C).

To test whether binding of Ca<sup>2+</sup> to both the C-terminal and the N-terminal lobes of CaM is necessary for activation of CaMKII under conditions that approximate those in the spine, we designed mutant CaMs that bind Ca<sup>2+</sup> only in the C- or N-terminal lobes: CaM-C<sup>WT</sup> and CaM-N<sup>WT</sup>, respectively (Fig. 2D and E and Table 1). Unlike previously reported mutant CaMs that are deficient in Ca<sup>2+</sup> binding because of point mutations of Ca<sup>2+</sup>-ligating residues (36, 41, 42), our mutant CaMs were designed to mimic intermediate conformations that CaM might adopt in the cytosol by specifically stabilizing the closed conformation of the mutant Ca<sup>2+</sup>-binding loops. We used the protein design program ORBIT (43), which employs an empirical atom-based force field and a fast side-chain selection algorithm to search through different protein sequences to find the lowest energy sequence for a given protein structure. To abolish Ca<sup>2+</sup> binding to a particular CaM domain, we redesigned the amino acid sequence of either the N-terminal or the C-terminal domain, leaving the other domain intact. For each calculation, a sequence of CaM residues forming the mutant Ca<sup>2+</sup>-binding site in the N- or C-terminal domain was optimized by using the Ca<sup>2+</sup>-free CaM structure as the template (ref. 33; Table 1). For each of these calculated sequences, we verified that the redesigned Ca<sup>2+</sup> site had fewer residues with Ca<sup>2+</sup> coordinating side chains.

**Assessment of Folding and Ca<sup>2+</sup> Binding by Mutant CaMs.** The designed mutant CaMs were expressed in *Escherichia coli* and assessed by far-UV circular dichroism for proper folding and Ca<sup>2+</sup> binding. In the absence of Ca<sup>2+</sup>, both mutant CaMs retain a predominantly  $\alpha$ -helical structure essentially identical to that of WT CaM. Upon addition of Ca<sup>2+</sup>, both exhibit a small change in the circular dichroism signal, as does WT CaM, reflecting Ca<sup>2+</sup>-induced rearrangements of the EF-hand domains (Fig. 6, which is published as supporting information on the PNAS web site). Binding of Ca<sup>2+</sup> to the C-terminal sites has been shown to be responsible for most of these changes in circular dichroism spectrum (44). Consistent with that finding, the structural transition of our N-terminal mutant (CaM-C<sup>WT</sup>) is nearly identical to that of WT CaM (Fig. 6A and B).

We compared the Ca<sup>2+</sup> binding stoichiometry of WT and mutant CaMs by electrospray mass spectrometry as described in ref. 45. In the presence of EGTA, the spectra of WT CaM and mutant CaMs

contained a major peak corresponding to the molecular weight of the protein in the Ca<sup>2+</sup>-free state (data not shown). In the presence of saturating Ca<sup>2+</sup>, the WT CaM spectrum comprised a peak corresponding to Ca<sup>2+</sup>-free CaM and four additional peaks reflecting incremental additions of one Ca<sup>2+</sup> ion. The major peak corresponds to four bound Ca<sup>2+</sup> ions (Fig. 3A). For CaM-C<sup>WT</sup> and CaM-N<sup>WT</sup>, the major peaks correspond to one and two bound Ca<sup>2+</sup> ions, as expected (Fig. 3B and C).

We measured the Ca<sup>2+</sup>-binding affinities of the mutant CaMs employing the fluorescent calcium sensor Fluo4FF. When CaM competes with Fluo4FF for available Ca<sup>2+</sup>, the fluorescence signal is reduced (Fig. 3D). The concentrations of Ca<sup>2+</sup> and CaM over which the competition occurs reflect the affinity of CaM for Ca<sup>2+</sup>. The competition curves were fit with a four Ca<sup>2+</sup> site model for WT CaM and a two Ca<sup>2+</sup> site model for the mutant CaMs (46). Ca<sup>2+</sup>-binding affinities of WT and mutant CaMs range from 1 to

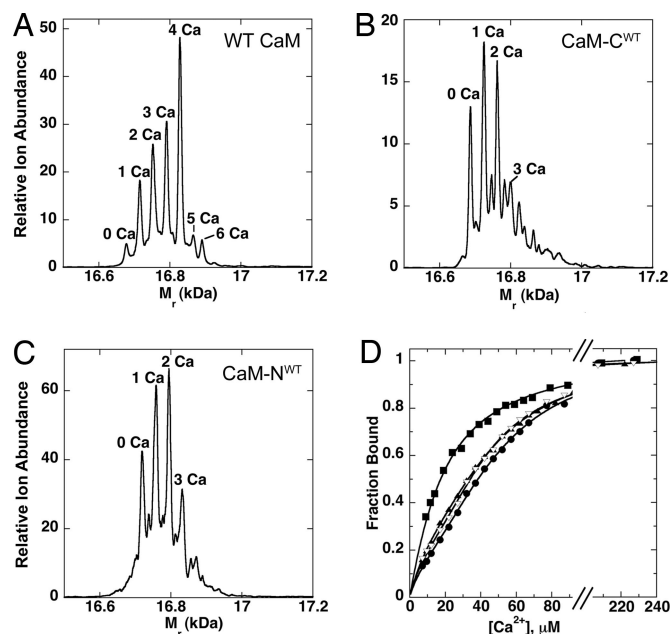


**Fig. 3.** High-affinity Ca<sup>2+</sup>-binding sites on WT and mutant CaMs. (A–C) Stoichiometry of Ca<sup>2+</sup> binding to WT and mutant CaMs measured by electrospray mass spectrometry at 10  $\mu$ M CaM and 200  $\mu$ M Ca<sup>2+</sup>. (A) WT CaM. (B) CaM-C<sup>WT</sup>. (C) CaM-N<sup>WT</sup>. (D) Ca<sup>2+</sup> binding to WT and mutant CaMs measured in a competition assay with the fluorescent Ca<sup>2+</sup>-binding dye, Fluo4FF. Ca<sup>2+</sup> was titrated into a solution of Fluo4FF (10  $\mu$ M) alone (●), Fluo4FF plus 10  $\mu$ M CaM-C<sup>WT</sup> (▽), 10  $\mu$ M CaM-N<sup>WT</sup> (▲), or 10  $\mu$ M WT CaM (■). The data were fit with a model assuming four high-affinity Ca<sup>2+</sup>-binding sites for WT CaM, two for CaM-C<sup>WT</sup> and CaM-N<sup>WT</sup>, and a single Ca<sup>2+</sup>-binding site for Fluo4FF (Table 2).

**Table 2. Kinetic properties of WT and mutant CaMs**

CaMs	$K_D$ values for $\text{Ca}^{2+}$ , $\mu\text{M}$				$K_{\text{act}}$ for CaMKII, $\mu\text{M}^2$	$k_p$ of CaMKII, $(\text{sec}^{-1})^3$
	$K_{D1}$	$K_{D2}$	$K_{D3}$	$K_{D4}$		
WT CaM	7.9	1.7	35	8.9	0.04	0.96
CaM-C <sup>WT</sup>	25	1.6	–	–	5	0.064
CaM-N <sup>WT</sup>	28	3.3	–	–	20	0.12

$K_D$  values for  $\text{Ca}^{2+}$  were calculated as described in *Methods* from the data in Fig. 3D with the Caligator program (47) downloaded from www.bpc.lu.se/research/caligator. A model containing four  $\text{Ca}^{2+}$  sites was used for WT CaM, and one containing two  $\text{Ca}^{2+}$  sites was used for CaM-C<sup>WT</sup> and CaM-N<sup>WT</sup>. The concentration of WT CaM required for half-maximal rate of CaMKII autophosphorylation,  $K_{\text{act}}$ , is taken from Meyer *et al.* (16).  $K_{\text{act}}$  values for mutant CaMs were determined from the data in Fig. 4B. The intrinsic turnover rate of CaMKII autophosphorylation,  $k_p$ , was determined from data in Fig. 5. Confidence intervals (95%) for  $k_p$  values were 0.67–1.25 for WT CaM, 0.044–0.084 for CaM-C<sup>WT</sup>, and 0.079–0.16 for CaM-N<sup>WT</sup>.

40  $\mu\text{M}$  (Table 2) and are in approximate agreement with previously published values for WT CaM (1, 36). The data reveal positive cooperativity between the two neighboring  $\text{Ca}^{2+}$ -binding sites in both mutant CaMs, as has been reported for WT CaM (1, 31). Thus, by several criteria, the two mutants behave as desired. In the presence of a saturating concentration of  $\text{Ca}^{2+}$ , CaM-C<sup>WT</sup> binds two  $\text{Ca}^{2+}$  ions in the C-terminal lobe, whereas CaM-N<sup>WT</sup> binds two  $\text{Ca}^{2+}$  ions in the N-terminal lobe.

We compared binding of WT and mutant CaMs to CaMKII-cbp at a saturating  $\text{Ca}^{2+}$  concentration by using circular dichroism to measure the coil-to-helix transition in the peptide upon binding, as previously described (ref. 48; Fig. 7, which is published as supporting information on the PNAS web site). Dissociation constants calculated by fitting the data to a 1:1 binding model show that WT CaM binds to CaMKII-cbp with a  $K_D$  of 5 nM, similar to values reported for other CaM-binding peptide sequences (48). In contrast, CaM-C<sup>WT</sup> binds with a  $K_D$  of 70 nM, and CaM-N<sup>WT</sup> binds with a much lower affinity  $K_D$  of 6  $\mu\text{M}$ .

**Activation of CaMKII by Mutant CaMs.** We tested whether the mutant CaMs support activation of CaMKII by measuring their ability to activate autophosphorylation at Thr-286. Unexpectedly, we found that, at saturating  $\text{Ca}^{2+}$  concentration, either of the mutant CaMs (10  $\mu\text{M}$ ) supports substantial autophosphorylation of CaMKII in a 1-min reaction (Fig. 4A). This result means that CaM does not require  $\text{Ca}^{2+}$  bound to both of its lobes to activate CaMKII. The  $K_{\text{act}}$  values for CaM-C<sup>WT</sup> and CaM-N<sup>WT</sup> under these conditions were 5 and 20  $\mu\text{M}$ , respectively (Fig. 4B), compared with a  $K_{\text{act}}$  value of  $\approx 50$  nM for WT CaM with four bound  $\text{Ca}^{2+}$  (Table 2). These results are consistent with the higher affinity of CaM-C<sup>WT</sup> for CaMKII-cbp and indicate that the binding of 2  $\text{Ca}^{2+}$  ions to the C-terminal lobe of WT CaM results in more effective activation of CaMKII than binding of two  $\text{Ca}^{2+}$  ions to the N-terminal lobe.

To explore the ability of the mutant CaMs to activate CaMKII under conditions closer to those believed to exist in postsynaptic spines during synaptic activity, we measured autophosphorylation of CaMKII while varying  $\text{Ca}^{2+}$  concentration from 0 to 10  $\mu\text{M}$  in the presence of 5  $\mu\text{M}$  CaM. Autophosphorylation of CaMKII in the presence of CaM-C<sup>WT</sup> was first detectable at  $\approx 1$   $\mu\text{M}$   $\text{Ca}^{2+}$  and in the presence of CaM-N<sup>WT</sup> at  $\approx 5$   $\mu\text{M}$   $\text{Ca}^{2+}$  (Fig. 4C). The rate of autophosphorylation was half-maximal at 2  $\mu\text{M}$   $\text{Ca}^{2+}$  for WT CaM, at 6  $\mu\text{M}$   $\text{Ca}^{2+}$  for CaM-C<sup>WT</sup>, and at  $>32$   $\mu\text{M}$   $\text{Ca}^{2+}$  for CaM-N<sup>WT</sup>. We then measured activation of CaMKII by each mutant CaM while varying their concentrations from 0.5 to 20  $\mu\text{M}$  in 12  $\mu\text{M}$   $\text{Ca}^{2+}$ . Under these conditions, WT CaM had a  $K_{\text{act}}$  of  $<0.4$   $\mu\text{M}$ , CaM-C<sup>WT</sup>  $\approx 7$   $\mu\text{M}$ , and CaM-N<sup>WT</sup>  $>30$   $\mu\text{M}$  (Fig. 4D). These results show that, in the presence of  $\text{Ca}^{2+}$ , both CaM-C<sup>WT</sup>, which mimics WT CaM with two  $\text{Ca}^{2+}$  ions bound at its C terminus (CaM2C), and CaM-N<sup>WT</sup>, which mimics WT CaM with two  $\text{Ca}^{2+}$  ions bound

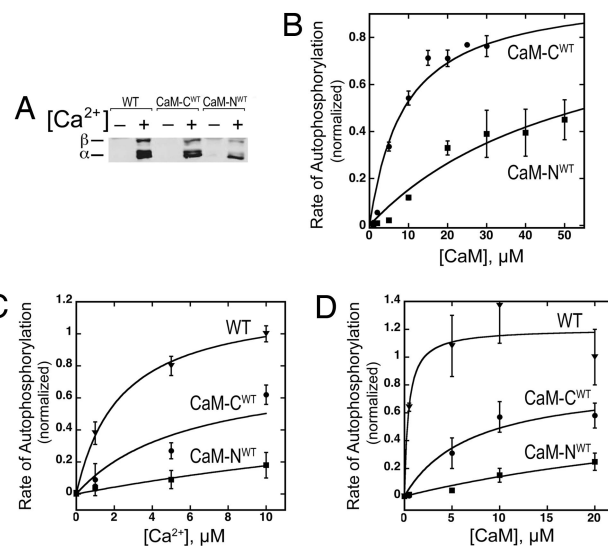


**Fig. 4.** Activation of autophosphorylation of CaMKII by WT and mutant CaMs. (A) Reactions were performed with 10  $\mu\text{M}$  CaM and 0.28  $\mu\text{M}$  CaMKII subunits for 1 min in the absence (–) or presence (+) of 300  $\mu\text{M}$   $\text{Ca}^{2+}$ , as described in *Methods*. The positions of  $\alpha$  and  $\beta$  subunits of CaMKII are indicated. (B) Dependence of autophosphorylation on the concentration of mutant CaMs. Autophosphorylation was performed as in A, except reactions were performed for 30 sec. To determine the  $K_{\text{act}}$  values reported in Table 2, the data were normalized to the level of autophosphorylation in saturating  $\text{Ca}^{2+}$ /CaM for 1 min and fit with a model assuming binding of 1 CaM to 1 catalytic subunit. (C) Dependence of autophosphorylation on  $\text{Ca}^{2+}$  in the presence of WT and mutant CaMs. Reactions were performed as in A, except with 5  $\mu\text{M}$  CaM, and quantified as in B. (D) Dependence of autophosphorylation on CaM concentration in the presence of 12  $\mu\text{M}$   $\text{Ca}^{2+}$ , and quantified as in B. Mean  $\pm$  SD of four experiments. WT ( $\blacktriangledown$ ), CaM-C<sup>WT</sup> ( $\bullet$ ), and CaM-N<sup>WT</sup> ( $\blacksquare$ ).

at the N terminus (CaM2N), can bind to and partially activate CaMKII *in vitro* under conditions, approximating those in stimulated postsynaptic spines. The results suggest that CaM2C is far more effective than CaM2N at binding and activating CaMKII in low concentrations of  $\text{Ca}^{2+}$ .

We performed quench flow experiments to measure the turnover rates of autophosphorylation supported by WT and mutant CaMs at their saturating concentrations. The turnover rate supported by either mutant was  $\approx 10\%$  of that supported by WT CaM (Table 2 and Fig. 5), suggesting that binding of the mutant CaMs cannot produce the optimal conformational change required for a maximal rate of autophosphorylation. We conclude that both mutant CaMs support activation and autophosphorylation of CaMKII; however, their affinity for CaMKII is lower than that of WT CaM, and they support a lower enzymatic turnover number.

## Discussion

We used a computational method to design mutant CaM proteins that bind two  $\text{Ca}^{2+}$  ions at either the N- or C terminus. At the inactivated terminus, we designed mutations that stabilize the closed structure of the  $\text{Ca}^{2+}$ -binding loop favored when  $\text{Ca}^{2+}$  is not bound (33, 37, 38). We used these mutants to study how CaM with  $\text{Ca}^{2+}$  bound to only one of its two lobes (CaM2C or CaM2N) interacts with its target protein CaMKII. These interactions are of interest because the direction of the changes in synaptic strength that occur during storage of information in neural circuits is exquisitely sensitive to small changes in the concentration of postsynaptic  $\text{Ca}^{2+}$  that occur during repetitive electrical activity (6, 8). This sensitivity to  $\text{Ca}^{2+}$  occurs at concentrations at which the equilibrium concentration of CaM2C (reached in  $\approx 50$  msec) is the same or higher than the concentration of WT CaM with  $\text{Ca}^{2+}$  ions

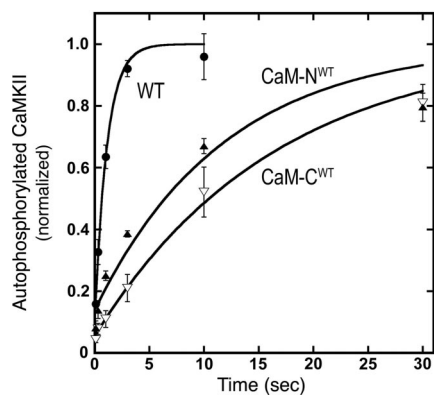


**Fig. 5.** Determination of turnover number for autophosphorylation of CaMKII in the presence of WT and mutant CaMs. The time course of autophosphorylation of CaMKII was determined in saturating  $\text{Ca}^{2+}$ /CaM. Data were gathered with a Quench Flow apparatus and normalized as described in *Methods*, then fit with the equation:  $A(1 - e^{-k_p(t - t_0)})$ , where  $k_p$  is the turnover rate (unknown),  $t_0$  (a negative term) is the time at which the extrapolated autophosphorylation curve crosses the  $x$  axis (*Supporting Text*), and  $A$  is a scaling factor.  $A$ ,  $k_p$ , and  $t_0$  were fit simultaneously by nonlinear regression performed with the Levenberg–Marquardt method in Mathematica. The  $k_p$  values supported by each form of CaM are summarized in Table 2. Data were obtained from five experiments with WT CaM, five with CaM- $\text{C}^{\text{WT}}$ , and three with CaM- $\text{N}^{\text{WT}}$ . WT CaM (●), CaM- $\text{C}^{\text{WT}}$  (▽), and CaM- $\text{N}^{\text{WT}}$  (▲).

bound at all four sites (CaM4), as determined by simulations of  $\text{Ca}^{2+}$  binding to free CaM under conditions present in spines (ref. 49 and unpublished observations). Furthermore, because the N-terminal lobe of CaM binds  $\text{Ca}^{2+}$  with  $\approx 10$ - to 100-fold higher  $k_{\text{on}}$  and  $k_{\text{off}}$  than the C-terminal lobe, as much as 20% of free CaM may be in the CaM2N conformation 5 msec after the onset of  $\text{Ca}^{2+}$  influx through NMDA receptors. Thus, competition for CaM2C or CaM2N within a synaptic spine may determine whether the synapse will be potentiated or depressed.

Using the values reported in this study we can estimate the relative concentrations of CaM2C·CaMKII, CaM2N·CaMKII, and CaM4·CaMKII when the  $\text{Ca}^{2+}$  concentration in the postsynaptic density is 0.5  $\mu\text{M}$  or 2  $\mu\text{M}$   $\text{Ca}^{2+}$  (S.M. and M.B.K., unpublished data). We assumed concentrations of 30  $\mu\text{M}$  CaMKII subunits and 10  $\mu\text{M}$  free CaM and a  $K_D$  of 50 nM for binding of CaM4 to CaMKII. At 0.5  $\mu\text{M}$   $\text{Ca}^{2+}$ , the concentration of CaM2C·CaMKII is  $\approx 0.8$   $\mu\text{M}$ , which is  $\approx 10$  times more than the concentration of CaM4·CaMKII. Because of the low affinity of CaM2N for CaMKII, its concentration is  $\approx 80$  times lower than the concentration of CaM2C·CaMKII. At 2  $\mu\text{M}$   $\text{Ca}^{2+}$ , the concentrations of CaM2C·CaMKII (2.3  $\mu\text{M}$ ) and CaM4·CaMKII (3.2  $\mu\text{M}$ ) are roughly equal; both still exceed CaM2N·CaMKII by a factor of 80. These numbers show that the enhanced affinity for the third and fourth  $\text{Ca}^{2+}$  ions bound to CaM when CaMKII is present results in formation of a significant amount of CaM4·CaMKII at 2  $\mu\text{M}$   $\text{Ca}^{2+}$ . However, this mechanism doesn't appear to account quantitatively for the substantial activation of autophosphorylation at concentrations of  $\text{Ca}^{2+}$  as low as 0.35  $\mu\text{M}$  (Fig. 1). We conclude that activation of CaMKII by binding of CaM2C alone likely contributes to activation of CaMKII during small increases in  $\text{Ca}^{2+}$  in the spine above the basal concentration of 80 nM such as might occur during low-frequency stimulation. This finding is consistent with the recently reported structural arrangement of the holoenzyme of CaMKII (22) (see *Supporting Text* and Fig. 8, which are published as supporting information on the PNAS web site). Our findings demonstrate the importance of understanding the kinetics of interactions of CaM2C and CaM2N with their various targets to correctly simulate the orchestration of biochemical responses to  $\text{Ca}^{2+}$  influx into the spine.

Previous studies have shown that the individual N- or C-terminal lobes of CaM with bound  $\text{Ca}^{2+}$  can activate certain effector proteins, phosphorylase kinase (50), myosin light chain kinase, neuronal nitric oxide synthase (51), and adenylate cyclase (52). These studies relied either on isolated N-terminal and C-terminal fragments of CaM generated by proteolysis (50, 51) or on point mutants of CaM that have lost one or more  $\text{Ca}^{2+}$ -binding sites (52). More recent studies have made use of CaM with single-point mutations in each of the two N-terminal sites (CaM<sub>12</sub>) or the two C-terminal sites (CaM<sub>34</sub>) to show that the individual lobes of CaM have distinct functional effects on voltage-activated  $\text{Ca}^{2+}$  channels (53, 54). Although these mutants have been useful for understanding the qualitative ability of individual CaM domains to interact with target proteins, they are not ideal for determining the actual binding constants of such interactions as they occur *in vivo*. The reason that single-point mutations or proteolytic fragmentation may introduce structural changes in CaM that do not represent its intermediate conformations in the cytosol. These changes may influence their rates of binding to targets (55). By stabilizing the mutated  $\text{Ca}^{2+}$ -binding loops of CaM in the structure assumed by apo-CaM, we have attempted to mimic as closely as possible the transient forms of CaM loaded with  $\text{Ca}^{2+}$  ions at either the N or C terminus. These mutant CaMs will be useful for understanding how  $\text{Ca}^{2+}$  controls mechanisms of synaptic plasticity that underlie learning and memory. They also may be useful for studying  $\text{Ca}^{2+}$ -signaling events in other cell types.

## Methods

**Computational Methods.** The sequences for the mutant CaMs were designed by using the protein design program ORBIT (ref. 43; see *Supporting Text*). The sequences of the N- and C-terminal CaM domains were optimized with the  $\text{Ca}^{2+}$ -free CaM structure as a template (33) to produce CaM- $\text{C}^{\text{WT}}$  and CaM- $\text{N}^{\text{WT}}$ , respectively.

**Expression of CaM Proteins.** cDNAs encoding CaM- $\text{C}^{\text{WT}}$  and CaM- $\text{N}^{\text{WT}}$  mutants were constructed with an inverse PCR procedure beginning with the WT CaM cDNA cloned into pET-15 (Novagen, San Diego, CA). WT and mutant CaMs were expressed and purified as described in ref. 56.

**Peptide Synthesis.** The CaMKII-cbp peptide corresponding to the CaM-binding domain of CaMKII (sequence -AKSKWKQAFNA-TAVVRHMRKQLQ-) was synthesized and purified in the Caltech Peptide Synthesis Facility as described in ref. 56.

**Electrospray Mass Spectrometry.** Electrospray ionization mass spectrometry was performed on an API365 LC/MS/MS system (PE SCIEX) with a nanospray ion source (Protana, Toronto, ON, Canada) operated at an infusion mode of 0.2  $\mu\text{l}/\text{min}$  and a spray voltage of  $-1.4$  kV. The data were collected in the negative ion mode. The  $\text{Ca}^{2+}$ -bound samples (10  $\mu\text{M}$  CaM) were diluted into 4 mM  $\text{NH}_4\text{HCO}_3/200$   $\mu\text{M}$   $\text{CaCH}_3\text{CO}_2/15\%$   $\text{CH}_3\text{OH}$ , pH 8.0. For the  $\text{Ca}^{2+}$ -free samples,  $\text{CaCH}_3\text{CO}_2$  was replaced with 500  $\mu\text{M}$  EGTA.

**$\text{Ca}^{2+}$ -Binding Affinities.**  $\text{Ca}^{2+}$  binding to WT and mutant CaMs was measured by competition with the  $\text{Ca}^{2+}$ -binding fluorescent dye Fluo4FF (Molecular Probes, Eugene, OR). We determined the intrinsic binding affinity of Fluo4FF for  $\text{Ca}^{2+}$  ( $K_D \approx 13$   $\mu\text{M}$ ) in the absence of CaM by titrating concentrated  $\text{CaCl}_2$  into a 10  $\mu\text{M}$  solution of Fluo4FF in 50 mM Tris/100 mM NaCl/1 mM  $\text{MgCl}_2$ , pH 7.2 at 25°C and recording fluorescence after addition of each aliquot of  $\text{Ca}^{2+}$  on a Hitachi (Tokyo, Japan) F-4500 fluorescence spectrophotometer (excitation at 488 nm and emission recorded at 516 nm). The measured fluorescence signal  $F$  was used to calculate the free  $\text{Ca}^{2+}$  concentration  $[\text{Ca}^{2+}]_{\text{free}}$ , the concentration of  $\text{Ca}^{2+}$  bound to the dye  $[\text{Ca}^{2+}\cdot\text{Dye}]$ , and the affinity of CaM for  $\text{Ca}^{2+}$  in the presence of targets as described in *Supporting Text*.

**CaMKII Autophosphorylation Assay.** Reactions were initiated by addition of purified CaMKII (0.28  $\mu\text{M}$ ) to a final volume of 100  $\mu\text{l}$  of 50 mM Tris/0.1 M NaCl<sub>2</sub>/0.9 mg/ml BSA/50  $\mu\text{M}$  ATP/5 mM DTE, pH 7.2, the desired concentration of WT or mutant CaM, and desired Ca<sup>2+</sup> concentration determined by mixing appropriate ratios of 100 mM CaCl<sub>2</sub> and 100 mM EGTA as described in instructions supplied with the Ca<sup>2+</sup> buffer kit (Molecular Probes, Carlsbad, CA). The buffer was warmed to 30°C for 1 min, reactions were initiated, proceeded for 1 min, and were stopped by the addition of 3% SDS/2% 2-mercaptoethanol. Samples containing 0.2  $\mu\text{g}$  of CaMKII were fractionated by SDS/PAGE, transferred by electrophoresis onto a nitrocellulose membrane for 1 h at 350 mA in 25 mM Tris base/0.2 M glycine/20% methanol. Membranes were immunoblotted with 7.5  $\mu\text{g}$  antibody 22B1 in 15 ml of 50 mM Tris, pH 7.4/0.5 M NaCl/0.05% Tween 20 (TTBS) plus 2% normal goat serum for 3 h at 4°C. Monoclonal antibody 22B1 (anti-phospho-CaMKII; Affinity Bioreagents, Golden, CO) is specific for  $\alpha$  and  $\beta$  subunits of CaMKII only when they are phosphorylated at Thr-286/287 (in  $\beta$ ). Bound antibodies were visualized by measuring fluorescence of a secondary antibody, (IRDye800-Anti-mouse; Rockland, Gilbertsville, PA; 1.5  $\mu\text{g}$  in 30 ml of TTBS) with an Odyssey Imaging System (Li-Cor Biosciences, Lincoln, NE). Conditions were adjusted so that fluorescence intensity was linear over the range of CaMKII measured. The amount of autophosphorylated CaMKII was calculated by quantifying the intensity of each band with the Odyssey software and normalizing it to the intensity of a band corresponding to standard fully autophosphorylated CaMKII prepared by incubating in the assay solution for 1 min with 300  $\mu\text{M}$  Ca<sup>2+</sup> and 10  $\mu\text{M}$  WT CaM.

**Measurement of Turnover Numbers for Autophosphorylation of CaMKII.** Initial rates of autophosphorylation were measured at saturating levels of Ca<sup>2+</sup>/CaM and ATP with the use of a temperature-controlled Kintek Model RQF-3 Quench Flow apparatus

(Kintek Corp., Austin, TX). Reactions were initiated at 100 ms, 300 ms, 1, 3, 10, and 30 sec by rapid mixing of solution 1 (25 mM Tris·HCl, pH 7.2/0.1 M NaCl/1 mM MgCl<sub>2</sub>/2 mM Ca<sup>2+</sup>/0.9 mg/ml BSA/5 mM DTE/1.4  $\mu\text{M}$  CaMKII catalytic subunits, and either 12  $\mu\text{M}$  WT CaM, 30  $\mu\text{M}$  CaM-C<sup>WT</sup>, or 60  $\mu\text{M}$  CaM-N<sup>WT</sup>) and solution 2 (identical to solution 1 except that CaMKII and CaM were replaced by 200  $\mu\text{M}$  ATP). The two solutions were kept at 4°C until they were transferred to the quench flow apparatus and warmed for 1 min to 30°C. Autophosphorylation was initiated by rapid mixing of 16  $\mu\text{l}$  of each solution and terminated by rapid addition of a final concentration of 1% SDS, 3.3 mM glycine·HCl, pH 2.9 (see *Supporting Text*) After quenching, all reactions were brought to a final concentration of 3% SDS, 66 mM Tris·HCl (pH 7.2)/2% 2-mercaptoethanol/5% glycerol/40  $\mu\text{g}/\text{ml}$  Bromophenol Blue and subjected to SDS/PAGE followed by immunoblotting with antibody 22B1 as described for the autophosphorylation assay. Intensities of autophosphorylated bands were quantified with the Odyssey Imaging System. The levels of autophosphorylation were normalized to that of fully autophosphorylated CaMKII incubated in the assay for 30 sec (WT CaM) or 100 sec (mutant CaMs). The amount of autophosphorylated CaMKII in each sample lane was obtained from a standard curve built for each set of experiments by measuring the intensity of 0.06, 0.12, and 0.23  $\mu\text{g}$  of fully autophosphorylated CaMKII and fitting the standard data with a power function.

We thank K. Beckingham (Rice University, Houston, TX) for providing a plasmid encoding calmodulin, E. Winfree and laboratory for the use of their spectrofluorometer, J. Oh and E. Marcora for CaMKII, A. Ingemar for help with CaLigand, and J. Zhou for help with mass spectrometry. This work was supported by the Howard Hughes Medical Institute, the Ralph M. Parsons Foundation, and an IBM Shared University research grant (to S.L.M.), the Sloan-Schwartz Foundation (to M.H.C.), and U.S. Public Health Service Grants NS047300 (to M.H.C) and NS44306 (to M.B.K.).

- Klee CB (1988) in *Calmodulin*, eds Cohen P, Klee CB (Elsevier, Amsterdam, The Netherlands), Vol 5, pp 35–56.
- Wang JH, Sharma RK, Huang CY, Chau V, Chock PB (1980) *Ann NY Acad Sci* 356:190–204.
- Burger D, Stein EA, Cox JA (1983) *J Biol Chem* 258:14733–14739.
- Olwin BB, Edelman AM, Krebs EG, Storm DR (1984) *J Biol Chem* 259:10949–10955.
- Xia Z, Storm DR (2005) *Nat Rev Neurosci* 6:267–76.
- Yang SN, Tang YG, Zucker RS (1999) *J Neurophysiol* 81:781–787.
- Abbott LF, Nelson SB (2000) *Nat Neurosci* 3(Suppl):1178–1183.
- Franks KM, Sejnowski TJ (2002) *BioEssays* 24:1130–1144.
- Bi GQ, Rubin J (2005) *Trends Neurosci* 28:222–228.
- Rubin JE, Gerkin RC, Bi GQ, Chow CC (2005) *J Neurophysiol* 93:2600–2613.
- Kennedy MB, Beale HC, Carlisle HJ, Washburn LR (2005) *Nat Rev Neurosci* 6:423–434.
- Lisman J, Schulman H, Cline H (2002) *Nat Rev Neurosci* 3:175–190.
- Quinlan EM, Halpain S (1996) *Neuron* 16:357–368.
- Mulkey RM, Endo S, Shenolikar S, Malenka RC (1994) *Nature* 369:486–488.
- Miller SG, Kennedy MB (1985) *J Biol Chem* 260:9039–9046.
- Meyer T, Hanson PI, Stryer L, Schulman H (1992) *Science* 256:1199–1202.
- Hudmon A, Schulman H (2002) *Annu Rev Biochem* 71:473–510.
- Hubbard MJ, Klee CB (1987) *J Biol Chem* 262:15062–15070.
- Klee CB, Cohen P (1988) in *Calmodulin*, eds Cohen P, Klee CB (Elsevier, Amsterdam, The Netherlands), pp 225–248.
- Lisman J (1989) *Proc Natl Acad Sci USA* 86:9574–9578.
- Bennett MK, Erondy NE, Kennedy MB (1983) *J Biol Chem* 258:12735–12744.
- Rosenberg OS, Deindl S, Sung RJ, Nairn AC, Kuriyan J (2005) *Cell* 123:849–860.
- Rosenberg OS, Deindl S, Comolli LR, Hoelz A, Downing KH, Nairn AC, Kuriyan J (2006) *FEBS J* 273:682–694.
- Hanson PI, Meyer T, Stryer L, Schulman H (1994) *Neuron* 12:943–956.
- Miller SG, Kennedy MB (1986) *Cell* 44:861–870.
- Miller SG, Patton BL, Kennedy MB (1988) *Neuron* 1:593–604.
- Giese KP, Fedorov NB, Filipkowski RK, Silva AJ (1998) *Science* 279:870–873.
- Watterson DM, Harrelson WG, Jr., Keller PM, Sharief F, Vanaman TC (1976) *J Biol Chem* 251:4501–4513.
- Erondy NE, Kennedy MB (1985) *J Neurosci* 5:3270–3277.
- Sabatini BL, Oertner TG, Svoboda K (2002) *Neuron* 33:439–452.
- Linse S, Helmersson A, Forsen S (1991) *J Biol Chem* 266:8050–8054.
- Yamniuk AP, Vogel HJ (2004) *Mol Biotechnol* 27:33–57.
- Kuboniwa H, Tjandra N, Grzesiek S, Ren H, Klee CB, Bax A (1995) *Nat Struct Biol* 2:768–776.
- Babu YS, Bugg CE, Cook WJ (1988) *J Mol Biol* 204:191–204.
- Wall ME, Clarage JB, Phillips GN (1997) *Structure (London)* 5:1599–612.
- Maune JF, Klee CB, Beckingham K (1992) *J Biol Chem* 267:5286–5295.
- Zhang M, Tanaka T, Ikura M (1995) *Nat Struct Biol* 2:758–767.
- Finn BE, Evenas J, Drakenberg T, Waltho JP, Thulin E, Forsen S (1995) *Nat Struct Biol* 2:777–783.
- Chin D, Means AR (2000) *Trends Cell Biol* 10:322–328.
- Meador WE, Means AR, Quijcho FA (1992) *Science* 257:1251–1255.
- Krueger JK, Bishop NA, Blumenthal DK, Zhi G, Beckingham K, Stull JT, Trewhella J (1998) *Biochemistry* 37:17810–17817.
- Peterson BZ, DeMaria CD, Adelman JP, Yue DT (1999) *Neuron* 22:549–558.
- Dahiyat BI, Mayo SL (1997) *Science* 278:82–87.
- Maune JF, Beckingham K, Martin SR, Bayley PM (1992) *Biochemistry* 31:7779–7786.
- Veenstra TD, Johnson KL, Tomlinson AJ, Naylor S, Kumar R (1997) *Biochemistry* 36:3535–3542.
- Wyman J, Gill SJ (1990) *Binding and Linkage: Functional Chemistry of Biological Molecules* (University Science Books, Mill Valley, CA).
- Andre I, Linse S (2002) *Anal Biochem* 305:195–205.
- Shifman JM, Mayo SL (2003) *Proc Natl Acad Sci USA* 100:13274–13279.
- Franks KM, Bartol TM, Sejnowski TJ (2001) *Neurocomputing* 38–40:9–16.
- Kuznicki J, Grabarek Z, Brzeska H, Drabikowski W, Cohen P (1981) *FEBS Lett* 130:141–145.
- Persechini A, McMillan K, Leakey P (1994) *J Biol Chem* 269:16148–16154.
- Gao ZH, Krebs J, VanBerkum MF, Tang WJ, Maune JF, Means AR, Stull JT, Beckingham K (1993) *J Biol Chem* 268:20096–20104.
- DeMaria CD, Soong TW, Alseikhan BA, Alvania RS, Yue DT (2001) *Nature* 411:484–489.
- Liang H, DeMaria CD, Erickson MG, Mori MX, Alseikhan BA, Yue DT (2003) *Neuron* 39:951–960.
- Mukherjee P, Beckingham K (1993) *Biochem Mol Biol Int* 29:555–563.
- Shifman JM, Mayo SL (2002) *J Mol Biol* 323:417–423.